Etching characteristics of high-kk dielectric HfO(2) thin films in inductively coupled fluorocarbon plasmas

Takahashi, Kazuo; Ono, Kouichi; Setsuhara, Yuichi

JVSTA Journal of Vacuum Science & Technology A

Etching characteristics of high- k dielectric Hf O 2 thin films in inductively coupled fluorocarbon plasmas

Kazuo Takahashi, Kouichi Ono, and Yuichi Setsuhara

Citation: Journal of Vacuum Science & Technology A **23**, 1691 (2005); doi: 10.1116/1.2073468
View online: http://dx.doi.org/10.1116/1.2073468
View Table of Contents: http://scitation.aip.org/content/avs/journal/jvsta/23/6?ver=pdfcov
Published by the AVS: Science & Technology of Materials, Interfaces, and Processing

Etching characteristics of high-*k* dielectric HfO_2 thin films in inductively coupled fluorocarbon plasmas

Kazuo Takahashi,[a] Kouichi Ono, and Yuichi Setsuhara[b]
Department of Aeronautics and Astronautics, Kyoto University, Yoshida-Honmachi, Sakyo-ku, Kyoto 606-8501, Japan

(Received 4 March 2005; accepted 15 August 2005; published 25 October 2005)

Inductively coupled fluorocarbon (CF_4/Ar and C_4F_8/Ar) plasmas were used to etch HfO_2, which is a promising high-dielectric-constant material for the gate of complementary metal-oxide-semiconductor devices. The etch rates of HfO_2 in CF_4/Ar plasmas exceeded those in C_4F_8/Ar plasmas. The tendency for etch rates to become higher in fluorine-rich (high F/C ratio) conditions indicates that HfO_2 can be chemically etched by fluorine-containing species. In C_4F_8/Ar plasmas with a high Ar dilution ratio, the etch rate of HfO_2 increased with increasing bias power. The etch rate of Si, however, decreasd with bias power, suggesting that the deposition of carbon-containing species increased with increasing the power and inhibited the etching of Si. The HfO_2/Si selectivity monotonically increased with increasing power, then became more than 5 at the highest tested bias power. The carbon-containing species to inhibit etching of Si play an important role in enhancing the HfO_2/Si selectivity in C_4F_8/Ar plasmas. © *2005 American Vacuum Society.* [DOI: 10.1116/1.2073468]

I. INTRODUCTION

As integrated-circuit device dimensions continue to be scaled down, increasingly strict requirements are being imposed on plasma etching technology. The requirements include the etch anisotropy, profile control, feature size, or critical dimension control relative to the mask layer, selectivity to the underlying layers and, also, microscopic uniformity of these etch parameters. For the gate etch process of a complementary metal-oxide-semiconductor (CMOS) device application, historically the two most important issues to be addressed have been a precise control of the profile and critical dimension of gate electrodes, and a high selectivity to gate oxides. In practice, the gate width of advanced devices is projected to be scaled down to much less than 100 nm, and the thickness of gate oxides is also reduced to 2 nm or less for the present material, SiO_2. The thickness reduction brings a number of serious problems such as increased gate leakage current and reduced oxide reliability.

Regarding gate dielectrics, the technological challenge continues for growing ultrathin SiO_2 films of high quality; however, the ultimate solution relies on high-dielectric-constant (k) materials. Recent efforts have been made to replace SiO_2 with silicon oxynitrides of slightly higher dielectric constant, and, nowadays, new high-k (>20) dielectrics, or metal oxides such as Al_2O_3, HfO_2, and ZrO_2, are being developed to replace SiO_2.[1–5] The metal oxides provide the required specific capacitance at a considerably larger thickness than SiO_2, thus allowing the reduction of gate leakage current. In integrating these materials into device fabrication, an understanding of the etching characteristics of high-k materials is required for their removal and for contact etching.

Plasma etching of metal oxides with a high k has been studied for the application of ferroelectric materials, buffer layers, and capacitor dielectrics. However, only a few studies have been concerned with the plasma etching of high-k materials for gate-dielectrics application. Pelhos *et al.* reported on the etching of high-k gate dielectric $Zr_{1-x}Al_xO_y$ thin films with helical resonator plasmas in BCl_3/Cl_2.[6] Sha *et al.* reported on the etching of ZrO_2 with electron cyclotron resonance plasmas in Cl_2 (Ref. 7) and BCl_3/Cl_2.[8] They also etched HfO_2 thin films in chlorine chemistries.[9,10] In their studies of HfO_2 etching, chlorine-based chemistries not fluorine were chosen, because in previous works,[11,12] HfO_2 etching stopped in CHF_3 plasmas, whereas the fluorinated Hf compound can be formed as sidewall masks. Moreover, Norasetthekul *et al.* reported on the etching of HfO_2 with inductively coupled plasmas in Cl_2/Ar, SF_6/Ar, and CH_4/H_2/Ar.[13] They concluded that the etch rates in Cl_2 were higher than those in SF_6/Ar.

An emphasis in these studies has been placed on etch chemistries giving the selectivity of more than one over the underlying Si substrate, as well as a better understanding of the corresponding physics and chemistry under processing. The thickness of the gate dielectrics for next-generation CMOS devices (in the 65 nm technology node and beyond) will be several nm. Therefore, selectivity to underlying layers or mask materials will be more important than the etch rate in the gate process.[14] From the point of view of HfO_2/Si selectivity, highly selective etching may be achieved in fluorocarbon plasmas, because a surface inhibitor of polymer probably sticks on Si that does not include oxygen.[15] In this paper we present results of the etching of HfO_2 thin films on Si substrates in inductively coupled fluorocarbon (CF_4/Ar and C_4F_8/Ar) plasmas. Then we discuss the performance of

[a]Electronic mail: takahashi@kuaero.kyoto-u.ac.jp
[b]Present address: Joining and Welding Research Institute, Osaka University, 11-1, Mihogaoka, Ibaraki, Osaka 567-0047, Japan.

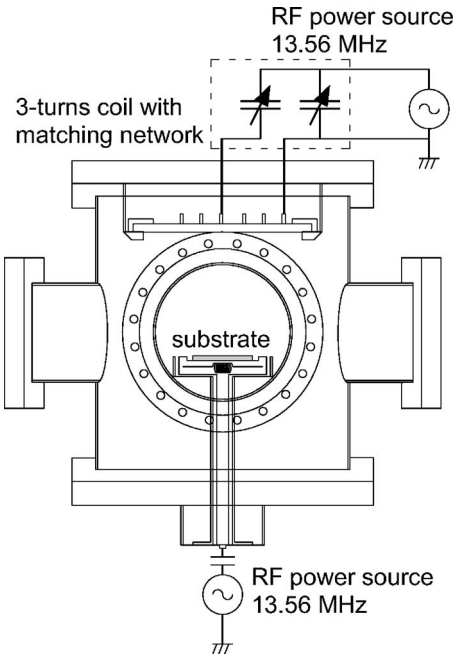

FIG. 1. Schematic of the reactor chamber.

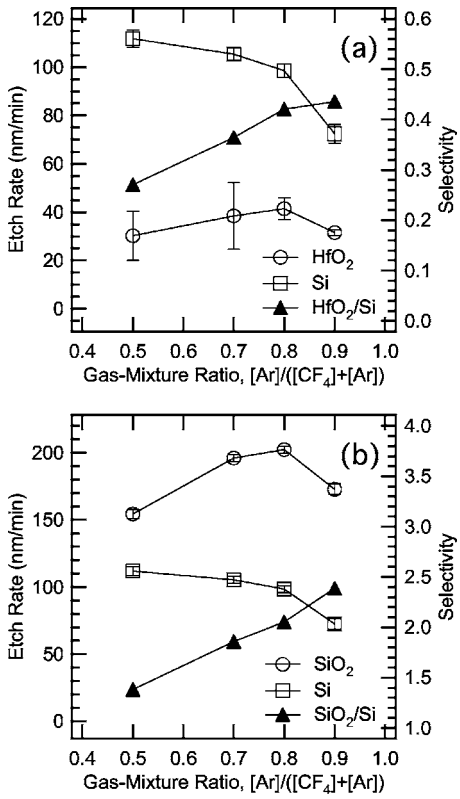

FIG. 2. Etch rates of (a) HfO_2 and (b) SiO_2 in CF_4/Ar plasmas plotted with that of Si, and etch selectivities of (a) HfO_2/Si and (b) SiO_2/Si as a function of gas–mixture ratio. The total gas flow rate, pressure, power to the coil, and rf bias power were 50 sccm, 20 mTorr, 280 W, and 50 W, respectively.

fluorocarbon plasmas in etching HfO_2 and try to understand the etch mechanism by comparing it with that of SiO_2, which is well known in previous works.[16]

II. EXPERIMENT

Samples for etching were 60 nm thick HfO_2 films on Si substrates prepared by chemical vapor deposition, SiO_2 films formed by thermal oxidation and bare Si substrates. The samples were cleaved into 2 cm^2 pieces and attached on a 4 in. diameter Si wafer, which was then clamped onto a wafer stage.

Etching experiments were performed in a low-pressure inductively coupled plasma (ICP) reactor supplied with 13.56 MHz rf power (Fig. 1). The reactor consisted of a grounded stainless-steel chamber 25 cm in diameter and 25 cm high. The rf power supply was coupled to the plasma via a three-turn planar rf induction coil 15 cm in outer diameter, positioned on a quartz window 20 cm in diameter and 1.2 cm thick, located at the top side of the chamber. The wafer stage was 13 cm in diameter, being located at the bottom side of the chamber, where a close-fitting ground shield surrounded the stage. The distance from the bottom edge of the rf coupling window to the wafer stage was 5 cm. Gas mixtures of CF_4/Ar and C_4F_8/Ar and pure Ar were introduced into the reactor evacuated to a base pressure $<1\times10^{-6}$ Torr, and the gas pressure was typically 20 mTorr at a flow rate of 50 or 250 sccm.

The discharge was established at a nominal rf power of 100–300 W, corresponding to net powers to the π-type matching circuit driving the induction coil. The wafer stage was capacitively coupled to a separate 13.56 MHz rf power supply for additional biasing; the rf bias power was varied between 10 and 150 W (net power), resulting in a dc self-bias voltage on the stage down to between −40 and −160 V.

Sample pieces covered with a Si wafer were etched for several minutes. Steps appeared on the sample pieces after removing the Si wafer. To determine etch rates, step height on the sample pieces was measured by stylus profilometry. For evaluating a real gate etch process of industrial applications, photoresist masks should be used. In the present study, the Si wafer was used as a mask to make experimental procedures more convenient. The basic aspect of etch characteristics, however, can be understood by using the Si masks.

The chemical composition of the surface was analyzed by x-ray photoelectron spectroscopy (XPS) using Mg $K\alpha$ x-ray radiation and a pass energy of 50 eV at a takeoff angle of 90°. A cylindrical Langmuir probe was placed 2 cm above the wafer stage to measure plasma parameters (ion density, electron temperature, and plasma potential).

III. RESULTS AND DISCUSSION

A. CF_4/Ar and C_4F_8/Ar plasmas

Figure 2(a) shows the etch rate of HfO_2 in CF_4/Ar plasmas as a function of the gas–mixture ratio [Ar]/([CF_4]+[Ar]) at constant rf powers of 280 W (to the coil) and 50 W (for bias), together with that of Si and the etch selectivity of HfO_2/Si. In generating the plasmas, the gas flow rate and the pressure were maintained at 50 sccm and

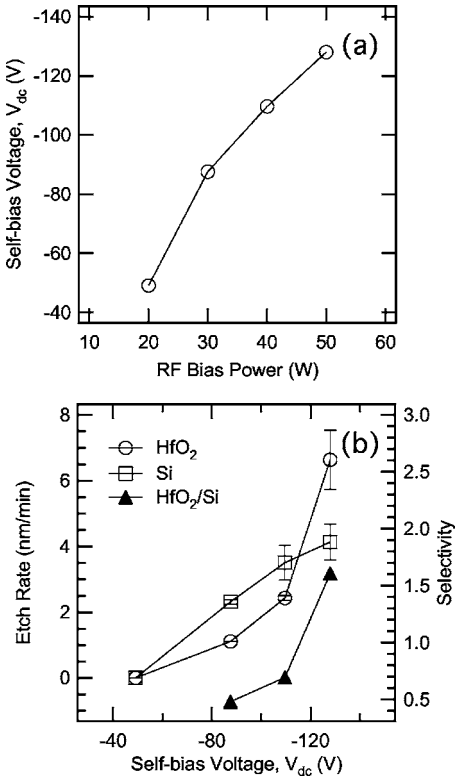

FIG. 3. (a) Self-bias voltage in pure Ar plasmas as a function of rf bias power, and (b) the etch rate of HfO_2 plotted with that of Si, and etch selectivity of HfO_2/Si as a function of self-bias voltage. The power to the coil was set at 120 W. The total gas flow rate and the pressure were the same as in Fig. 2.

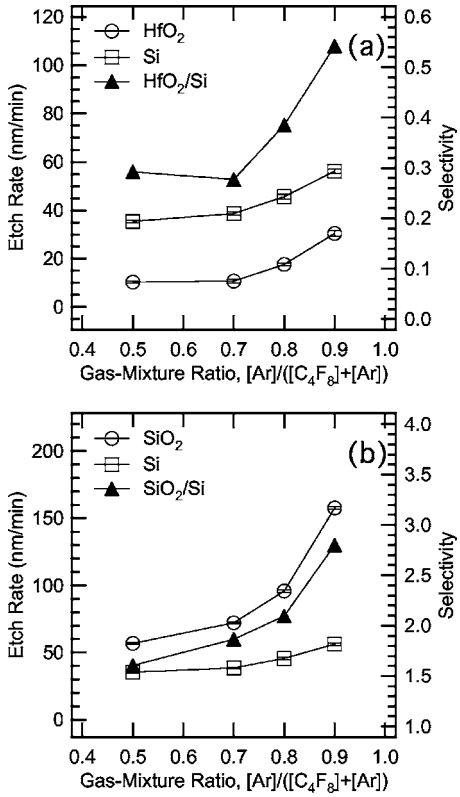

FIG. 4. Etch rates of (a) HfO_2 and (b) SiO_2 in C_4F_8/Ar plasmas plotted with that of Si, and etch selectivities of (a) HfO_2/Si and (b) SiO_2/Si as a function of the gas–mixture ratio. The experimental parameters were the same as in Fig. 2.

20 mTorr, respectively. Here the etched depth was measured as a function of the etch time up to several minutes, exhibiting an approximately linear increase with time; thus, the etch rate was calculated as the ratio of the depth to time.

The etch rate of Si decreased with an increasing gas–mixture ratio, indicating that the amount of fluorine radicals or etchants for Si decreases with decreasing [CF_4]. The etch rate of HfO_2 was not changed so much. The result was that the selectivity was enhanced with increasing [Ar]. The dc self-bias voltage on the wafer stage was reduced (from −160 to −110 V) with increasing [Ar], implying that the bombarding ion energy was decreased with increasing [Ar]. The ion density, however, increased slightly with increasing [Ar]. The ion flux should have been kept almost constant in the tested regime of the gas–mixture ratio. If the ion flux maintained the etch rate of HfO_2, one can guess that Ar ion sputtering contributes to HfO_2 etching.

Assuming the etch mechanism of HfO_2 to mainly be sputtering by ion bombardment, the samples were then exposed to pure Ar plasmas at a constant power of 120 W (to the coil) and bias power was varied between 10 and 50 W. The gas flow rate and pressure were 50 sccm and 20 mTorr, respectively. The dc self-bias voltage increased with increasing bias power [Fig. 3(a)]. Then the etch rates of HfO_2 and Si increased with increasing the selfbias voltage [Fig. 3(b)]. At a bias power of 50 W, the rate of HfO_2 was higher than that of Si (HfO_2/Si selectivity >1). Furthermore, the etch rate was no more than 10 nm/min even at a constant power increased to 280 W (to the coil). The rate was half as high as that in CF_4/Ar plasmas. Therefore, the etching of HfO_2 may be caused not only by ion sputtering, but also, by chemical reactions in CF_4/Ar plasmas.

The etching characteristics of SiO_2 were also examined in the CF_4/Ar plasmas [Fig. 2(b)]. The etch rate increased with increasing [Ar] in the range of the gas–mixture ratio from 0.5 to 0.8, and then decreased. The dependence of the SiO_2 etch rate on the gas–mixture ratio was similar to that of the HfO_2 etch rate, rather than that of Si. Therefore, the etch mechanism of HfO_2 may be partly understood on the analogy of that of SiO_2. The etching of SiO_2 can proceed with dissociation of the Si–O bond in the reaction of fluorocarbon radicals on the surface activated by ion bombardment,[17] e.g.,

$$SiO_2 + CF_x \rightarrow SiF_4\uparrow + COF_2\uparrow. \quad (1)$$

Similarly, fluorocarbon species and ion impact on the surface may also play an important role in HfO_2 etching. Moreover, the reaction involving fluorocarbon species can be effective, not for Si etching, but for protecting Si surfaces.[17]

Assuming the same chemistry as selective etching of SiO_2 over Si in fluorocarbon plasmas,[18,19] the carbon-rich compound of C_4F_8 was employed for HfO_2 etching. Generally, C_4F_8 plasmas can produce more fluorocarbon species contributing to SiO_2 etching and protect the Si surface than CF_4 plasmas.[20,21] Consequently, the fluorine radical as a etchant

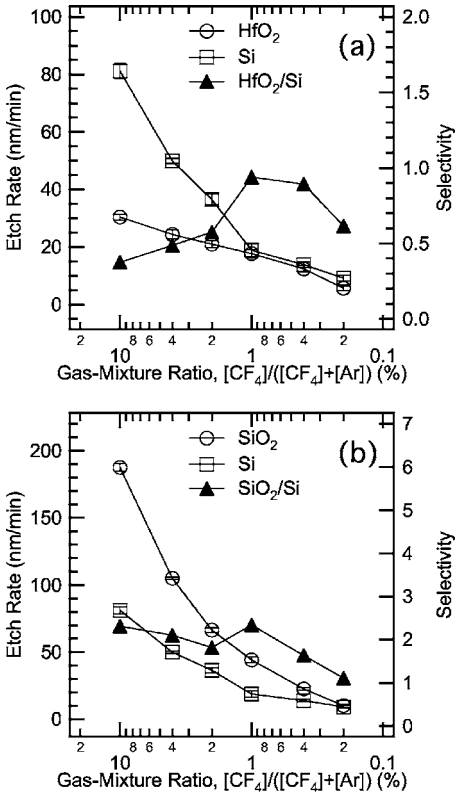

FIG. 5. Etch rates of (a) HfO_2 and (b) SiO_2 in C_4F_8/Ar plasmas with a high Ar dilution ratio plotted with that of Si, and etch selectivities of (a) HfO_2/Si and (b) SiO_2/Si as a function of the gas–mixture ratio. The total gas flow rate, pressure, power to the coil, and rf bias power were set at 250 sccm, 20 mTorr, 280 W, and 50 W, respectively.

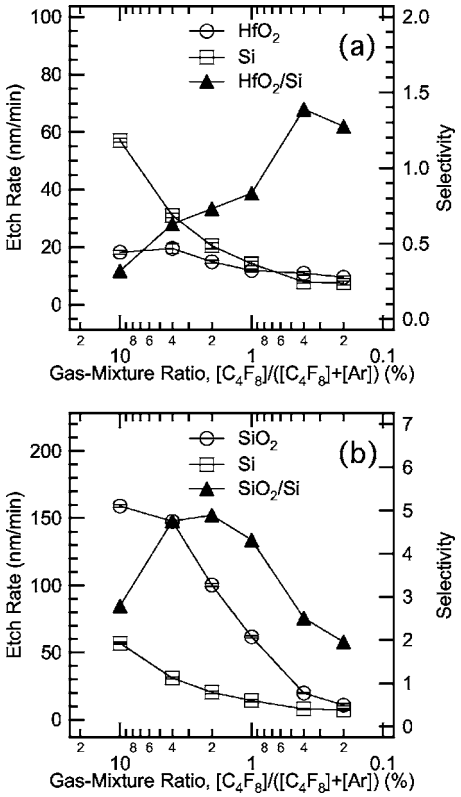

FIG. 6. Etch rates of (a) HfO_2 and (b) SiO_2 in C_4F_8/Ar plasmas with a high Ar dilution ratio plotted with that of Si, and etch selectivities of (a) HfO_2/Si and (b) SiO_2/Si as a function of the gas–mixture ratio. The experimental parameters were the same as in Fig. 5.

in Si etching becomes a relatively minor product in C_4F_8 plasmas, and HfO_2/Si selectivity is expected to be higher in comparison with CF_4 plasmas. Figure 4 shows the etch rates of HfO_2, SiO_2, and Si, and the selectivities of HfO_2/Si and SiO_2/Si in C_4F_8/Ar plasmas. The etch rate of Si was reduced in comparison with CF_4/Ar plasmas. At the highest gas–mixture ratio, the HfO_2/Si selectivity slightly exceeded that in CF_4/Ar plasmas. Because the self-bias voltage decreased with increasing [Ar], the etching was enhanced not by increasing ion impact energy, but by the chemical reaction involving fluorocarbon species in C_4F_8 plasmas, as well as in CF_4/Ar plasmas. Furthermore, the etch rate of HfO_2 being higher in fluorine-rich conditions (in the CF_4 plasmas) implies that HfO_2 can be etched by fluorine with changing into fluoride etch products, although melting and sublimation points of transition-metal fluoride are over a few hundred °C (the sublimation point of HfF_4 is 970 °C).[22] Because fluorine was detected on the HfO_2 surface exposed to CF_4/Ar and C_4F_8/Ar plasmas in the XPS measurements, as mentioned in the next section, it was possible that hafnium fluoride (HfF_x) was formed in our cases.

On the other hand, there was no conspicuous advantage in the SiO_2/Si selectivity obtained in the C_4F_8 plasmas. Because the etch rates of SiO_2 in the C_4F_8 plasmas were lower than those in the CF_4 plasmas, the fluorine radical, not fluorocarbon species, seemed to work mainly in SiO_2 etching, as well as in Si etching. Therefore, the reduction of the etch rate of Si in the C_4F_8/Ar plasmas resulted from the reduction of fluorine content; as a result, the HfO_2/Si selectivity improved in the plasmas.

To obtain a higher selectivity of HfO_2/Si, one must suppress Si etching with depositing a surface inhibitor (fluorocarbon polymer) and enhance HfO_2 etching caused by fluorocarbon radicals. Assuming that the Hf–O bond can be dissociated in the same chemistry as SiO_2 etching, requiring much bombarding by Ar ions,

$$HfO_2 + CF_x \rightarrow HfF_4\uparrow + COF_2\uparrow, \tag{2}$$

it would be necessary to increase the CF_x radical densities and ion flux activating the reactions on the surface. Therefore, the conditions with a high Ar dilution ratio, which are preferable for SiO_2/Si selective etching,[23,24] were employed in the present study.

Figure 5 shows the etch rates of HfO_2, SiO_2, and Si, and the selectivities of HfO_2/Si and SiO_2/Si in CF_4/Ar plasmas with a high Ar dilution ratio. Figure 6 shows those values for the case of C_4F_8/Ar plasmas. In these experiments, the total flow rate was increased to 250 sccm, and other conditions, powers, pressure, and so on were the same as the former experiments. The etch rates of HfO_2 and Si decreased with an increasing Ar dilution ratio in both the CF_4/Ar and C_4F_8/Ar plasmas [Figs. 5(a) and 6(a)]. The tendency seems to indicate that the etch mechanism gradually changed from

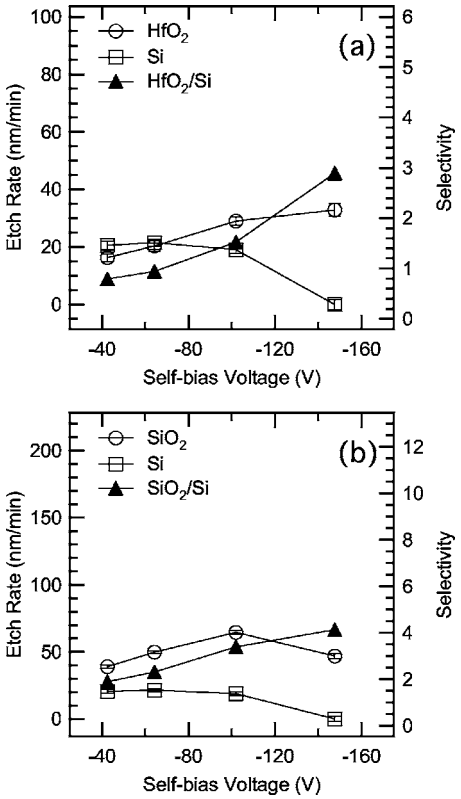

FIG. 7. Etch rates of (a) HfO_2 and (b) SiO_2 in $CF_4(1\%)/Ar$ plasmas with high Ar dilution ratio plotted with that of Si, and etch selectivities of (a) HfO_2/Si and (b) SiO_2/Si as a function of self-bias voltage. The gas–mixture ratio of $[CF_4]$ to the total was maintained at 1%. The etching was performed at 20 mTorr, 280 W (to the coil), and 50 W (for bias).

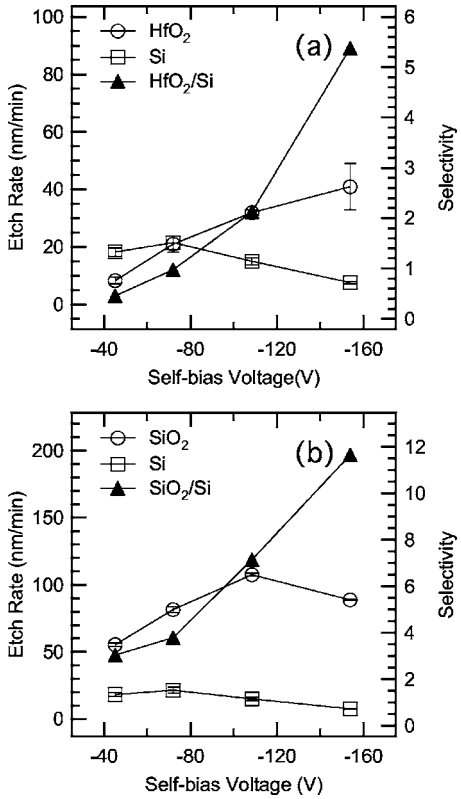

FIG. 8. Etch rates of (a) HfO_2 and (b) SiO_2 in $C_4F_8(1\%)/Ar$ plasmas with a high Ar dilution ratio plotted with that of Si, and etch selectivities of (a) HfO_2/Si and (b) SiO_2/Si as a function of self-bias voltage. The gas-mixture ratio of $[C_4F_8]$ to the total was maintained at 1%. The etching was performed in the same condition as in Fig. 7.

chemical etching to physical sputtering with increasing [Ar]. In the C_4F_8/Ar plasmas, the HfO_2/Si selectivity became more than unity at the gas-mixture ratios of 0.2, and 0.4% close to the pure Ar plasma condition. In contrast, in CF_4/Ar plasmas, the HfO_2/Si selectivity could not be more than unity.

In SiO_2 etching [Figs. 5(b) and 6(b)], the etch rate of SiO_2 decreased with increasing [Ar] in the same way as the cases of HfO_2 and Si. The SiO_2/Si selectivity in the C_4F_8 plasmas rises to the peak at the gas–mixture ratio of 2%, and that in the CF_4 plasmas keeps under 2.5 over all the tested gas–mixture ratios. In the C_4F_8 plasmas, SiO_2 must have been chemically etched by an etchant of the fluorocarbon species (not fluorine radical) in the conditions around the peak. Nevertheless there was no peculiarity in the tendency of the HfO_2 etch rate, indicating that the reactions caused by bombarding ions were dominant in the mechanism of the HfO_2 etching. Besides, it can be safely said that HfO_2 can be etched, in part, by chemically reactive species such as the fluorine radical, as mentioned above. The chemical etching of HfO_2 will be an important means of controlling the etch profile, because the profile formed in the chemical will be better for device manufacturing than that in the Ar ion sputtering process only.

B. Increasing rf bias power

The results mentioned above show that HfO_2 can be etched by chemical reactions appearing in the fluorine-rich conditions such as CF_4/Ar plasmas and by physical sputtering. From the point of view of etch profile control, one of the best solutions for the HfO_2 etching in fluorocarbon plasmas must be practical use of energetic ion bombardment with chemically reactive species. Therefore, HfO_2 samples were treated with increasing rf bias power to enhance bombarding Ar ion energy in CF_4/Ar and C_4F_8/Ar plasmas, where the flow rates of the fluorocarbon gases were maintained at a constant of 1%. Figures 7 and 8 show the etch rates of HfO_2, Si, and SiO_2, and the selectivities of HfO_2/Si and SiO_2/Si as a function of the self-bias voltage changed by rf bias power between 50 and 150 W in CF_4/Ar and C_4F_8/Ar plasmas, respectively. The etch rate of HfO_2 increased with increasing self-bias voltage, in other words, with enhancing Ar ion bombarding energy. The etch rate of SiO_2 increased with increasing voltage and reached saturation. The rate of Si decreased slightly with increasing voltage after increasing and reaching saturation. The selectivities of HfO_2/Si and SiO_2/Si in the C_4F_8/Ar plasma were higher than those in the CF_4/Ar plasma. In the C_4F_8/Ar plasma, the HfO_2/Si selectivity was more than 5.

The chemical compositions on etched surfaces were analyzed by XPS to understand the dependence of etch rates on

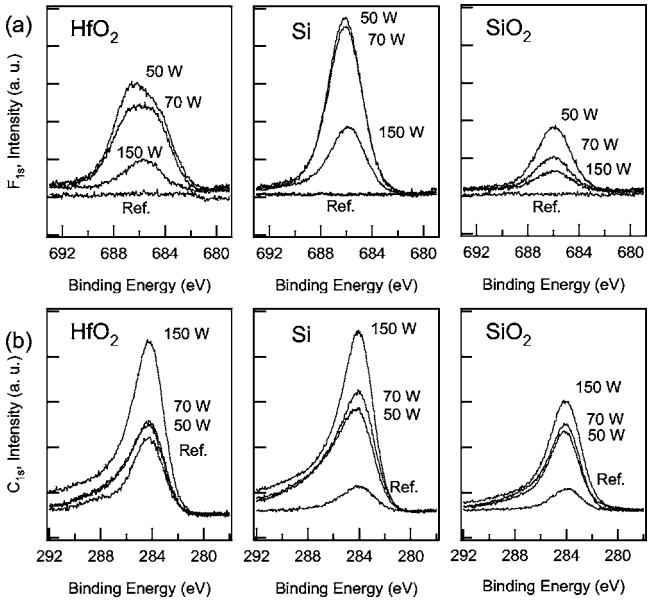

FIG. 9. XPS spectra of F_{1s} and C_{1s} on HfO_2, Si and SiO_2 surfaces etched in the C_4F_8 plasmas. The experimental parameters were the same as in Fig. 8. The rf bias power conditions are shown in the graphs. The values of 50, 70, and 150 W correspond to the self-bias voltages of −45, −72, and −154 V, respectively.

self-bias voltage. Figure 9 shows the XPS spectra of F_{1s} and C_{1s} on HfO_2, Si, and SiO_2 surfaces etched in C_4F_8/Ar plasmas, and on pre-etched surfaces (indicated by the notation of "Ref."). The experimental parameters were the same as in Fig. 8. Each graph shows the spectrum corresponding to the rf bias power condition (50, 70, and 150 W). The carbon content on pre-etched surfaces can be detected from adventitious hydrocarbon of atmospheric contaminants. On each surface, the intensity of the F_{1s} peak decreased with increasing rf bias power, and that of the C_{1s} peak increased. Thus, increasing rf bias power enhanced the deposition reaction of carbon, implied because the surface reaction probability for deposition can be higher with a higher energy of ion into the surface.[25] On HfO_2 and SiO_2 surfaces, the etching reaction may be proceeded with the formation of volatile etch products containing C and O atoms. On the Si surface without O atoms, however, the deposition of C atoms prevented the etching of the surface. Therefore, the selectivities of HfO_2/Si and SiO_2/Si increased with increasing rf bias power in C_4F_8/Ar plasmas (Fig. 8).

To understand the etch mechanism, the etch rates of HfO_2, Si, and SiO_2 were measured, depending on ion energy. Figure 10 shows the etch rates in C_4F_8/Ar plasmas at coil powers of 200 and 300 W. Here, the ion energy was defined by $|V_p - V_{dc}|$, where V_p and V_{dc} correspond to plasma potential measured by Langmuir probe and self-bias voltage, respectively. The gas flow rate and the pressure were set at 250 sccm and 20 mTorr, respectively. The gas–mixture ratio of $[C_4F_8]$ to the total was maintained at 1%. The ion density (N_i) and electron temperature (T_e) were also measured by a Langmuir probe and changed with power to the coil, as shown in Table I. The N_i became two times higher when the

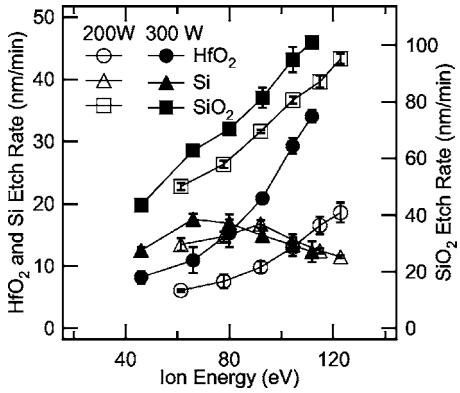

FIG. 10. Etch rates of HfO_2, Si, and SiO_2 in C_4F_8/Ar plasmas at the powers to the coil of 200 and 300 W as a function of ion energy. The gas flow rate and the pressure were set at 250 sccm and 20 mTorr, respectively. The gas–mixture ratio of $[C_4F_8]$ to the total was maintained at 1%.

power was increased from 200 to 300 W. The T_e, however, was maintained at a constant. The etch rate of Si did not change much, even with changes of ion energy and N_i, and implied that the deposition of C atoms prevented the etching of the Si surface. The etch rate of SiO_2 increased with increasing ion energy, and became 1.2 times higher with increasing N_i. Furthermore, the etch rate of HfO_2 increased with increasing ion density, and HfO_2 etching could be two times faster with increasing N_i. This result indicates that HfO_2 can be etched by an ion-assisted reaction and ion sputtering.

IV. CONCLUSION

The etch characteristics of HfO_2 were examined in CF_4/Ar and C_4F_8/Ar plasmas. The etch rate of HfO_2 tends to be high in fluorine-rich (e.g., CF_4/Ar) plasmas and where there is abundant Ar ion bombardment of the surface (e.g., CF_4/Ar and C_4F_8/Ar plasmas with high Ar dilution ratio, and with high self-bias voltage). These results indicated that HfO_2 could be etched both chemically by fluorine radical and physically by Ar ion bombardment. This was confirmed by the dependence of the HfO_2 etch rate on ion energy and ion density.

Here, we consider the application of fluorocarbon plasmas to actual gate etch processes. In physical sputtering without chemical reactions, redeposition of sputtered atoms makes the etch profile worse. Hence, an etch process involving chemical reactions with volatile etch products is required. The gate materials should be etched by fluorine-containing reactive species with ion bombardment. For HfO_2/Si selectivity greater than unity, it was necessary to increase the

TABLE I. Ion density (N_i) and electron temperature (T_e) depending on power to the coil.

Power (W)	N_i (cm^{-3})	T_e (eV)
200	1.1×10^{11}	2.9
300	1.9×10^{11}	2.8

HfO_2 etch rate and decrease the Si etch rate. This situation was produced in C_4F_8/Ar plasmas with high Ar dilution ratio and high self-bias power, and the HfO_2/Si selectivity of more than 5 was obtained.

In the present study, the same concept in the SiO_2/Si selective etching was applied to the HfO_2/Si selective etching, based on understanding previous works.[16] We do not understand all the chemistries for HfO_2 etching. For further qualified etching with high selectivity, it will be significant to use a fluorocarbon polymer efficiently, increasing surface inhibitors for Si etching.

ACKNOWLEDGMENT

This work was supported by the New Energy and Industrial Technology Development Organization (NEDO)/ Millennium Research for Advanced Information Technology (MIRAI) project.

[1]M. Hirose, Oyo Butsuri **71**, 1091 (2002) (in Japanese).
[2]A. Toriumi, T. Horikawa, and T. Nabetame, *Nikkei Microdevices Dec.*, 2002, p. 164 (in Japanese).
[3]G. D. Wilk and R. M. Wallace, Appl. Phys. Lett. **74**, 2854 (1999).
[4]M. Copel, M. Gribelyuk, and E. Gusev, Appl. Phys. Lett. **76**, 436 (2000).
[5]W.-J. Qi, R. Nieh, E. Dharmarajan, B. H. Lee, Y. Jeon, L. Kang, K. Onishi, and J. C. Lee, Appl. Phys. Lett. **77**, 1704 (2000).
[6]K. Pelhos, V. M. Donnelly, A. Kornblit, M. L. Green, R. B. Van Dover, L. Manchanda, Y. Hu, M. Morris, and E. Bower, J. Vac. Sci. Technol. A **19**, 1361 (2001).
[7]L. Sha, B.-O. Cho, and J. P. Chang, J. Vac. Sci. Technol. A **20**, 1525 (2002).
[8]L. Sha and J. P. Chang, J. Vac. Sci. Technol. A **21**, 1915 (2003).
[9]L. Sha, R. Puthenkovilakam, Y.-S. Lin, and J. P. Chang, J. Vac. Sci. Technol. B **21**, 2420 (2003).
[10]L. Sha and J. P. Chang, J. Vac. Sci. Technol. A **22**, 88 (2004).
[11]K. K. Shih, T. C. Chieu, and D. B. Dove, J. Vac. Sci. Technol. B **11**, 2130 (1993).
[12]J. A. Britten, H. T. Nguyen, S. F. Falabella, B. W. Shore, and M. D. Perry, J. Vac. Sci. Technol. A **14**, 2973 (1996).
[13]S. Norasetthekul, P. Y. Park, K. H. Baik, K. P. Lee, J. H. Shin, B. S. Jeong, V. Shishodia, D. P. Norton, and S. J. Pearton, Appl. Surf. Sci. **187**, 75 (2002).
[14]K. Ono, *2004 Semiconductor Technology Outlook*, 2004, p. 331 (in Japanese).
[15]T. Maeda, H. Ito, R. Mitsuhashi, A. Horiuchi, T. Kawahara, A. Muto, T. Sasaki, K. Torii, and H. Kitajima, Jpn. J. Appl. Phys., Part 1 **43**, 1864 (2004).
[16]M. Sekine, Appl. Surf. Sci. **192**, 270 (2002).
[17]R. A. Heinecke, Solid-State Electron. **18**, 1146 (1975).
[18]R. A. Heinecke, Solid-State Electron. **19**, 1039 (1976).
[19]L. M. Ephrath, J. Electrochem. Soc. **126**, 1419 (1979).
[20]S. Matsuo and Y. Adachi, Jpn. J. Appl. Phys., Part 2 **21**, L4 (1982).
[21]K. Miyata, M. Hori, and T. Goto, J. Vac. Sci. Technol. A **14**, 2343 (1996).
[22]D. R. Lide, *CRC Handbook of Chemistry and Physics*, 79th ed. (CRC Press, Boca Raton, FL, 1998).
[23]H. Hayashi, K. Kurihara, and M. Sekine, Jpn. J. Appl. Phys., Part 1 **35**, 2488 (1996).
[24]N. Ikegami, A. Yabata, G. L. Liu, H. Uchida, N. Hirashita, and J. Kanamori, Jpn. J. Appl. Phys., Part 1 **37**, 2337 (1998).
[25]T. Tatsumi, M. Matsui, M. Okigawa, and M. Sekine, J. Vac. Sci. Technol. B **18**, 1897 (2000).